

Multiple ionization of neon by soft x-rays at ultrahigh intensity

R Guichard^{1,2}, M Richter³, J-M Rost¹, U Saalmann¹, A A Sorokin^{3,4,5}
and K Tiedtke⁴

¹ Max-Planck-Institut für Physik komplexer Systeme, Nöthnitzer Straße 38, D-01187 Dresden, Germany

² UPMC Université Paris 06, UMR 7614, Laboratoire de Chimie Physique Matière et Rayonnement, F-75005 Paris, France

³ Physikalisch-Technische Bundesanstalt, PTB, Abbestraße 2-12, D-10587 Berlin, Germany

⁴ Deutsches Elektronen-Synchrotron, DESY, Notkestraße 85, D-22603 Hamburg, Germany

⁵ Ioffe Physico-Technical Institute, Polytekhnicheskaya 26, 194021 St Petersburg, Russia

E-mail: roland.guichard@upmc.fr and mathias.richter@ptb.de

Received 31 January 2013, in final form 9 April 2013

Published 13 August 2013

Online at stacks.iop.org/JPhysB/46/164025

Abstract

At the free-electron laser FLASH, multiple ionization of neon atoms was quantitatively investigated at photon energies of 93.0 and 90.5 eV. For ion charge states up to 6+, we compare the respective absolute photoionization yields with results from a minimal model and an elaborate description including standard sequential and direct photoionization channels. Both approaches are based on rate equations and take into account a Gaussian spatial intensity distribution of the laser beam. From the comparison we conclude that photoionization up to a charge of 5+ can be described by the minimal model which we interpret as sequential photoionization assisted by electron shake-up processes. For higher charges, the experimental ionization yields systematically exceed the elaborate rate-based prediction.

(Some figures may appear in colour only in the online journal)

With the construction of x-ray lasers over the last few years, applying the free-electron laser (FEL) concept of self-amplified spontaneous emission [1–4], a number of experiments have become feasible which elucidate the principles of photon–matter interaction in a new parameter regime ([5, 6] and references therein). The combination of high frequency and high intensity allowed in particular new insight into the photoelectric effect and the photoionization process [7–15]. Even simple photoionization involves, in a strict sense, multi-electron dynamics as soon as the photoelectron is not ejected dominantly from the highest occupied orbital rendering a comprehensive theoretical description difficult. For more complex atomic targets such as xenon, multi-photon absorption in the energy range of the giant resonance poses in addition the question as to which role collective electron excitations play in the high-frequency–high-intensity domain [10, 16]. Due to these difficulties, the role of different processes for the understanding of multi-photon ionization in the x-ray regime has not been settled to date [16–20]. Hence, it is worthwhile to carefully assess in which cases simple processes, such as sequential photoionization, describe

the experiments quantitatively and where deviations ask for explanations with a more involved dynamics. In the VUV-regime it was found in an experiment with argon atoms that sequential ionization describes the measured yields for different charge states well [21]. In the hard x-ray regime, it could be shown that sequences of single ionization in inner electron shells describe photon–matter interaction for light elements such as neon (Ne) well [12]. The present work determines, in a combined experimental–theoretical study, the extent to which a sequential description for Ne is also valid in the EUV regime. For this purpose, results of ion spectroscopy on Ne atoms obtained in a focused beam of the FEL FLASH in Hamburg [1, 22] at photon energies of 93.0 and 90.5 eV are compared with a minimal analytical model for the sequential ionization we have developed and with recent theoretical results from a more elaborated rate-based approach, including besides energetically allowed sequential also direct channels [20]. We find that the sequential minimal model describes the first five ionization stages reasonably well. The cross sections for higher charged ions, where sequential ionization can be

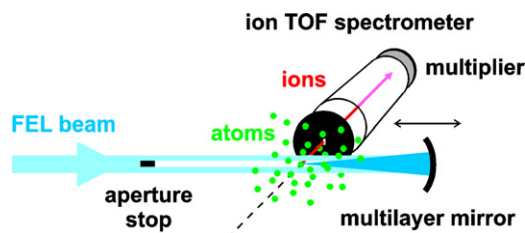


Figure 1. Experimental setup for the investigation of atoms by ion TOF spectroscopy in an FEL focus of a spherical narrow-bandwidth multilayer mirror.

excluded, are systematically underestimated by the elaborate rate description.

The experiments were carried out by applying ion time-of-flight (TOF) spectroscopy as shown in figure 1 [10, 18, 24]. The FEL beam was focused by the use of a spherical Si/Mo narrow-bandwidth multilayer mirror under normal incidence at the end of the beamline BL2 with a focal length of 20 cm and a reflectance between 60% and 70% [25], depending on the photon energy and confirmed with a relative standard uncertainty of 10%. The minimum focus diameter as small as $d_{\text{FWHM}} = (2.6 \pm 0.5) \mu\text{m}$ was derived from the target depletion effect [24]. The absolute FEL pulse energy in the μJ regime was monitored with a relative standard uncertainty of 15% on a shot-to-shot basis by means of calibrated gas-monitor detectors [26]. The photon energy was measured with the help of a grazing incidence spherical grating spectrometer [23] placed in front of all beamlines and a plane grating monochromator integrated in the beamline PG [22] before and after each measurement. The bandwidth of the FEL pulse was 1% to 1.5%. The mirror could be moved along the FEL beam in order to shift the focus in back-reflection geometry into and out of the interaction volume of our ion TOF spectrometer to vary the effective FEL beam cross section [10, 14]. As a result, the peak intensity (irradiance) of the FEL pulses with pulse durations of $\Delta t_{\text{FWHM}} = (15 \pm 5) \text{ fs}$ [16] could be varied from 10^{13} to $4 \times 10^{15} \text{ W cm}^{-2}$ and measured with a standard uncertainty of 42%. Ne filled the experimental vacuum chamber homogeneously at the low pressure of about 10^{-4} Pa to avoid any interaction between neighbouring atoms and ions. The pressure was measured by a calibrated spinning rotor gauge and the temperature by a calibrated Pt100 resistance thermometer. The homogeneous electric extraction field was sufficiently high to collect and register all ions generated within the interaction volume of the TOF spectrometer by an open electron multiplier operated in the analogue mode, i.e., by measuring the charge accumulated on the multiplier anode. The entrance aperture of the spectrometer had an extension of $350 \mu\text{m}$ in the beam direction and 1 mm perpendicular to the FEL beam. In front of the experimental chamber, a horizontal beam stop of 1.5 mm in height was introduced which enabled us to diaphragm ions produced by the incident unfocused beam (cf figure 1). TOF spectra were averaged over typically 500 consecutive FEL shots with pulse-to-pulse intensity fluctuations varying from 35% to 45%.

Figure 2 shows typical ion TOF spectra of Ne taken at the highest and lowest intensity level, corresponding to the regimes of multi- and single-photon excitations, respectively.

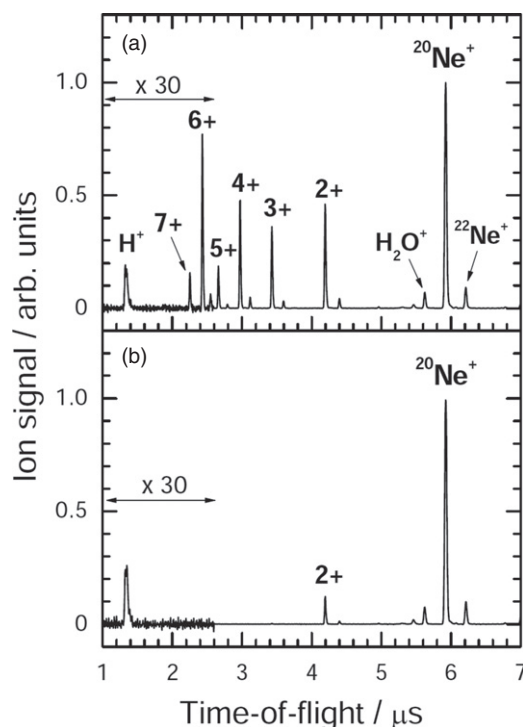


Figure 2. Ion TOF spectra of Ne taken at the photon energy of 93.0 eV and the peak intensity of (a) $4 \times 10^{15} \text{ W cm}^{-2}$ and (b) $2 \times 10^{13} \text{ W cm}^{-2}$. In the TOF regime below $2.6 \mu\text{s}$, the ion intensities were multiplied by a factor of 30.

Charged states up to 7+ were observed. Up to 6+, i.e., up to the complete removal of the 2p electron shell, the corresponding ionization yields were deduced from the ion signals by normalization to the absolute ion detection efficiency and to the number of target atoms within the interaction volume. The absolute detection efficiencies for singly charged ions were directly measured at low-intensity levels where single-photon excitation is dominating, using well-known photoionization cross section data of Ne ([26] and references therein). The detection efficiencies for higher charge states were deduced from those of singly charged ions assuming that the efficiency is proportional to the ion impact velocity [27, 28]. The number of target atoms was calculated from the interaction volume and the atomic particle density n_a . The latter was determined by $n_a = p/kT$, where p is the target gas pressure, T is the temperature and k is the Boltzmann constant. The interaction volume was calculated taking into account the minimum focus diameter, the distance of the interaction volume of the TOF spectrometer from the focus, the width of the spectrometer entrance aperture and the focused beam divergence. The latter was obtained using the known focal length of the mirror and measuring the size of the unfocused beam incident on the mirror. The relative standard uncertainty for the ionization yield is estimated to amount to 36% which arises from the uncertainties for the target density (2%), interaction volume (30%) and detection efficiency (20%). Figure 3 shows the experimental ionization yields for the Ne charge states from 1+ to 6+ as a function of the peak intensity, with squares and triangles for measurements at photon energies of 93.0 eV and 90.5 eV, respectively.

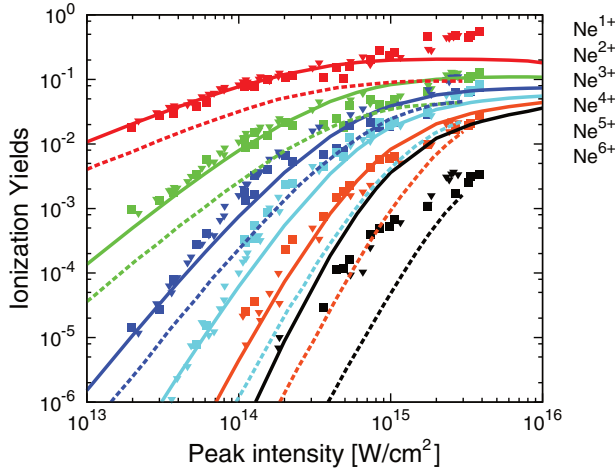


Figure 3. Experimental data for Ne ionization yields measured at photon energies of 93.0 (■) and 90.5 eV (▼) with pulses of 15 fs duration compared with results from the present minimal model (—) and results from the elaborate rate description for 30 fs pulse length of [20] (---).

The dependence of the different ionization yields on the peak intensity was also calculated by means of a minimal analytical model which is based on the stepwise removal of electrons by the sequential absorption of photons, i.e., $\text{Ne} \xrightarrow{\hbar\omega} \text{Ne}^+ \xrightarrow{\hbar\omega} \dots \xrightarrow{\hbar\omega} \text{Ne}^{n+}$, through a set of rate equations [29]

$$\dot{N}_0(t) = -\sigma_{01}F(t)N_0(t), \quad (1a)$$

$$\dot{N}_1(t) = \sigma_{01}F(t)N_0(t) - \sigma_{12}F(t)N_1(t), \quad (1b)$$

$$\dot{N}_2(t) = \sigma_{12}F(t)N_1(t) - \sigma_{23}F(t)N_2(t), \quad (1c)$$

⋮

with $F(t) = F_0f(t)$ where F_0 is the peak photon flux per unit area and $f(t)$ the dimensionless temporal shape of the photon pulses. σ_{jk} denotes the single-photon ionization cross section from the charge state j to k . With the new time variable

$$\tau(t) = \int_{-\infty}^t dt' f(t'), \quad (2)$$

which corresponds for infinite time to an effective pulse length $\tau_\infty = \tau(t \rightarrow \infty)$, the set of equations (1) may be rewritten as

$$\frac{d\mathbf{N}(I, \tau)}{d\tau} = \mathbf{M} \mathbf{N}(I, \tau), \quad (3)$$

with the *time-independent* matrix

$$\mathbf{M} = \frac{I}{\hbar\omega} \begin{pmatrix} -\sigma_{01} & 0 & \dots & 0 & 0 \\ +\sigma_{01} & -\sigma_{12} & \dots & 0 & 0 \\ 0 & +\sigma_{12} & \dots & 0 & 0 \\ \vdots & \vdots & & \vdots & \vdots \\ 0 & 0 & \dots & +\sigma_{n-1,n} & 0 \end{pmatrix} \quad (4)$$

and $\mathbf{N}(I, \tau) \equiv \{N_0(I, \tau), N_1(I, \tau), N_2(I, \tau), \dots\}^\dagger$ where the photon flux F_0 is replaced by the peak intensity $I = F_0 \hbar\omega$. The formal solution now reads

$$\mathbf{N}(I, \tau) = \exp(\mathbf{M}\tau) \mathbf{N}(0). \quad (5)$$

With the initial condition $\mathbf{N}(\tau=0) \equiv \mathbf{N}(t \rightarrow -\infty) = \{1, 0, 0, \dots\}^\dagger$, the vector components $N_{n>0}(I, \tau)$ may be

Table 1. Single-photon cross sections σ_{jk} in units of 10^{-18} cm^2 , from experiment [26, 30] (bold), using the GIPPER code⁶ [31] (italic) and a fitting procedure [32].

σ_{01}	σ_{12}	σ_{23}	σ_{34}
4.5	<i>4.07</i>	<i>3.98</i>	<i>3.71</i>
	4.31	4.55	3.96

interpreted as the respective ionization probabilities while $N_0(I, \tau)$ is the remaining fraction of neutral atoms.

From this general sequential ionization description we arrive at our minimal model by using identical cross sections $\sigma_{jk} = \sigma$ for all jk , i.e., we need only a single external parameter σ . For the first ionization steps, the use of identical step-wise cross sections can be justified since σ_{01} , σ_{12} , σ_{23} and σ_{34} , available in the 90–95 eV photon energy range, do not vary by more than 12% from their mean value of about $4.2 \times 10^{-18} \text{ cm}^2$ as can be seen in table 1.

In this minimal model one can solve (3) analytically with the explicit expression

$$N_n(I, \tau_\infty) = \frac{\lambda^n}{n!} \exp(-\lambda), \quad \lambda = \sigma I \tau_\infty / \hbar\omega. \quad (6)$$

For comparison with the experimental results, the theoretical data have to be convoluted with the spatial intensity distribution of the focused FEL beam within the interaction volume. We have chosen

$$I(I_0, r, z) = \frac{I_0}{1 + (z/z_R)^2} \exp\left(-\frac{2r^2}{w_0^2 [1 + (z/z_R)^2]}\right), \quad (7)$$

i.e., a Gaussian distribution in the radial direction r . Its standard deviation increases with z along the beam from the value $w_0 = d_{\text{FWHM}}/2\sqrt{\ln 2/2} = 2.208 \mu\text{m}$ at $z = 0$ while $z_R = 0.13 \text{ mm}$ denotes the estimated Rayleigh length of the focus for our experiments. The results of the minimal model according to equation (6) (with $\sigma = 4.2 \times 10^{-18} \text{ cm}^2$, $\tau_\infty = \sqrt{\pi/4 \ln 2} \Delta t_{\text{FWHM}} = 16 \text{ fs}$, $\hbar\omega = (93.0 + 90.5)/2 \text{ eV}$) convoluted with the spatial intensity distribution of equation (7) are shown as a function of the peak intensity I with solid lines in figure 3. For comparison, also the results of the elaborate rate description of the Ne ionization yields are shown by dashed lines [20].

As can be seen in figure 3, the experimental ion yields from Ne^{1+} to Ne^{5+} are well reproduced by our minimal analytical model with the parameter λ from equation (6) globally scaled by a factor 1.20 within the experimental uncertainties for λ of about 26%. The agreement between experimental data and the minimal model within the experimental uncertainties demonstrates both, the sequential character of the first few ionization steps and that the photon intensity distribution of equation (7) is appropriate for the spatial averaging. The discrepancies between experiment and the minimal model at high intensity ($> 10^{15} \text{ W cm}^{-2}$) might be explained by out-of-focus radiation, due to spherical aberrations, hitting the neutral atoms which are continuously distributed within the vacuum chamber.

The predictions of the elaborate rate description from [20] for the Ne^{1+} , Ne^{2+} and Ne^{3+} yields are of the same order of

⁶ Available on the Los Alamos website.

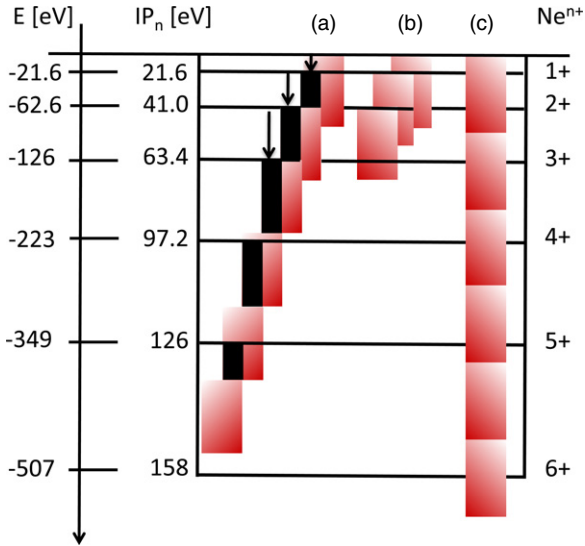


Figure 4. Different sequential photo ionization schemes for neon with 90.5 eV photons (red rectangles): (c) sequential ionization without respecting atomic structure, (b) only energetically allowed ionization steps from the respective ionic ground states, (a) sequential ionization with maximum photon energy storage through shake-up indicated by black rectangles. On the left the absolute energy scale of the neon ions (charge state on the right) are given; the ionization potentials IP_n in the middle for stepwise ionization from the respective ionic ground state are taken from [33].

magnitude, although a bit lower. This is most likely due to the fact that the laser pulse length is with 30 fs longer than that in the experiment (15 fs) or due to the different way of spatial averaging⁷. Mainly responsible for the ion yields is sequential ionization, since direct ionization does not play a significant role for the present parameters as can be inferred from [20]. However, only the first three sequential ionization steps which are energetically possible from the ground state of the respective ion (see (b) in figure 4) are taken into account. Therefore, the yields for Ne^{4+} and higher charged ions from [20] are significantly lower than the measured yields.

On the other hand, the minimal model captures the yields for Ne^{4+} and Ne^{5+} quite well, while overestimating the yield of Ne^{6+} . This can be understood from the sequential ionization scenario (a) with shake-up in figure 4: in the first ionization steps $IP_n \ll \hbar\omega$ such that a lot of photon energy is ‘waisted’ if one assumes ionization from the respective ionic ground state. However, through shake-up into various excited ion configurations it is possible to simultaneously excite the ion. The maximum photon energy J_n which can be stored in a photo ionization step n is given by the energy IP_{n+1} up to which an excited state of the $(n+1)$ -fold charged ion can exist. This energy might not be reached, if the photon energy is not sufficient, therefore $J_n = \min(E_n^{exs}, IP_{n+1})$ with

$$E_n^{exs} = \hbar\omega - IP_n - J_n + J_{n-1}. \quad (8)$$

Starting with $n = 1$ and $J_0 = 0$, equation (8) defines a recursive series for sequential photoionization with energy stored in shaken up electrons. The stored energy is indicated by black

⁷ Details of the rate calculations can be found in the supplement to [20], available online.

rectangles in figure 4. The arrows indicate ionization steps where $J_n = IP_{n+1}$, otherwise $J_n = E_n^{exs}$.

The series should continue until $E_n^{exs} < 0$. In neon, this is the case for $n = 6$ (see figure 4). Indeed, as can be seen from the experimental results in figure 3, the Ne^{6+} yield is much lower than predicted by the minimal sequential model which is, according to our analysis, only applicable for $n \leq 5$, but beyond the sequential ionization steps $n \leq 3$ used so far based on sequential ionization from ionic ground states.

To summarize, the reasonable agreement between experiment and theory for the yields of ions with lower charge gives confidence in the experiment and its actual parameters. The validity of our minimal model for sequential ionization up to charge states Ne^{5+} as demonstrated by comparison with the experiment is expected based on simple energy conservation arguments if energy storage in excited ions through shake-up processes is taken into account. Finally, the disagreement for higher ionic charges, here for Ne but also for Xe in the same range of photon energy [10, 18], suggests the existence of ionization routes beyond that of the sequential and direct pathways so far considered.

Acknowledgments

We thank the FLASH team for a very successful FEL operation. Support from the Deutsche Forschungsgemeinschaft (DFG RI 804/5-1) is gratefully acknowledged.

Appendix. Analytical solution to the coupled rate equations for sequential ionization

In the general case, the matrix \mathbf{M} in (5) reads

$$\mathbf{M} = \begin{pmatrix} -s_0 & 0 & \dots & 0 & 0 \\ +s_0 & -s_1 & \dots & 0 & 0 \\ 0 & +s_1 & \dots & 0 & 0 \\ \vdots & \vdots & & \vdots & \vdots \\ 0 & 0 & \dots & +s_{m-1} & 0 \end{pmatrix} \quad (A.1)$$

where the $s_i = \sigma_{i,i+1}F_0$ are the single-photon absorption rates for taking the ion from the charge state i to $i+1$. For simplicity, we have assumed a maximal charge state m . Thus, with the neutral fraction N_0 , the matrix \mathbf{M} has the size $(m+1) \times (m+1)$. After some algebra, one can find a transformation to the diagonal form

$$\tilde{\mathbf{M}} = \mathbf{T}^{-1}\mathbf{M}\mathbf{T} \quad (A.2a)$$

$$= \begin{pmatrix} -s_0 & 0 & \dots & 0 & 0 \\ 0 & -s_1 & \dots & 0 & 0 \\ \vdots & \vdots & & \vdots & \vdots \\ 0 & 0 & \dots & -s_{m-1} & 0 \\ 0 & 0 & \dots & 0 & 0 \end{pmatrix} \quad (A.2b)$$

with the transformation matrix

$$\mathbf{T} = \begin{pmatrix} 1 & 0 & \dots & 0 & 0 & 0 \\ P_0^0/Q_0^0 & 1 & \dots & 0 & 0 & 0 \\ P_0^1/Q_0^1 & P_1^1/Q_1^1 & \dots & 0 & 0 & 0 \\ \vdots & \vdots & \ddots & \vdots & \vdots & \vdots \\ P_0^{m-2}/Q_0^{m-2} & P_1^{m-2}/Q_1^{m-2} & \dots & P_{m-2}^{m-2}/Q_{m-2}^{m-2} & 1 & 0 \\ -P_1^{m-1}/Q_0^{m-2} & -P_2^{m-1}/Q_1^{m-2} & \dots & -P_{m-1}^{m-1}/Q_{m-2}^{m-2} & -1 & 1 \end{pmatrix} \quad (\text{A.3})$$

whereby the first two of the following products have been used:

$$P_k^l \equiv \prod_{i=k}^l s_i \quad Q_k^l \equiv \prod_{i=k}^l (s_{i+1} - s_k), \quad (\text{A.4a})$$

$$R_k^l \equiv \prod_{i=k}^l (s_{i-1} - s_l) \quad jS_k^l \equiv \prod_{i=k}^l (s_i - s_j). \quad (\text{A.4b})$$

The latter two will be used below. Note that $P_k^l = Q_k^l = R_k^l = 1$ for $k > l$. The denominators in the matrix elements of \mathbf{T} require that $s_0 \neq s_1 \neq s_2 \neq \dots \neq s_{m-1}$. The time evolution of the transformed system $\tilde{\mathbf{N}}(\tau) = \mathbf{T}^{-1}\mathbf{N}(\tau)$ is simply given by

$$\tilde{\mathbf{N}}(\tau) = \exp(\tau\tilde{\mathbf{M}})\tilde{\mathbf{N}}(0). \quad (\text{A.5})$$

In general, the initial condition is given by $\tilde{\mathbf{N}}(0) = \mathbf{T}^{-1}\mathbf{N}(0)$. For the particular form $\mathbf{N}(0) = \{1, 0, 0, \dots\}^\dagger$, it simplifies to

$$\tilde{N}_{n<m}(0) = P_0^{n-1}/R_1^n \quad (\text{A.6a})$$

$$\tilde{N}_m(0) = 1. \quad (\text{A.6b})$$

Finally, we can transform back to the original system by $\mathbf{N}(\tau) = \mathbf{T}\tilde{\mathbf{N}}(\tau)$ and obtain

$$\begin{aligned} N_{n<m}(\tau) &= \tilde{N}_n(\tau) + \sum_{j=0}^{n-1} \frac{P_j^{n-1}}{Q_j^n} \tilde{N}_j(\tau) \\ &= P_0^{n-1} \sum_{j=0}^n \frac{\exp(-s_j\tau)}{jS_0^n} \end{aligned} \quad (\text{A.7a})$$

$$N_m(\tau) = 1 - \sum_{j=0}^{m-1} N_j(\tau), \quad (\text{A.7b})$$

whereby we have used $P_0^{n-1} = P_0^{j-1}P_j^{n-1}$ and $jS_0^n = R_1^jQ_j^n$ in equation (A.7a) and $\sum_n N_n(\tau) \equiv 1$ in equation (A.7b). The

two equations (A.7) give the time-dependent probabilities N_n for the various charge states n .

For the minimal model discussed in the text, we need the expressions for degenerate absorption rates $s_0 = s_1 = s_2 = \dots = s$. These can be obtained by subsequent limits $s_0 \rightarrow s$, $s_1 \rightarrow s$, etc of equation (A.7a). One obtains the compact form

$$N_{n<m}(\tau) = \frac{(s\tau)^n}{n!} \exp(-s\tau) \quad (\text{A.8})$$

and $N_m(\tau)$ as in equation (A.7b).

References

- [1] Ackermann W *et al* 2007 *Nature Photon.* **1** 336
- [2] Shintake T *et al* 2008 *Nature Photon.* **2** 555
- [3] Emma P *et al* 2010 *Nature Photon.* **4** 641
- [4] David P *et al* 2011 *Nature Photon.* **5** 456
- [5] Bostedt C *et al* 2009 *Nucl. Instrum. Methods A* **601** 108
- [6] Berrah N *et al* 2010 *J. Mod. Opt.* **57** 1015
- [7] Wabnitz H *et al* 2002 *Nature* **420** 482
- [8] Siedschlag C *et al* 2002 *Phys. Rev. Lett.* **89** 173401
- [9] Saalmann U *et al* 2002 *Phys. Rev. Lett.* **89** 143401
- [10] Sorokin A A *et al* 2007 *Phys. Rev. Lett.* **99** 213002
- [11] Nagler B *et al* 2009 *Nature Phys.* **5** 693
- [12] Young L *et al* 2010 *Nature* **466** 56
- [13] Vinko S M *et al* 2012 *Nature* **482** 56
- [14] Richter M *et al* 2010 *J. Phys. B: At. Mol. Opt. Phys.* **43** 194005
- [15] Rudek B *et al* 2012 *Nature Photon.* **6** 857
- [16] Richter M 2011 *J. Phys. B: At. Mol. Opt. Phys.* **44** 075601
- [17] Makris M G *et al* 2009 *Phys. Rev. Lett.* **102** 033002
- [18] Richter M *et al* 2009 *Phys. Rev. Lett.* **102** 163002
- [19] Lambropoulos P *et al* 2011 *J. Phys. B: At. Mol. Opt. Phys.* **44** 175402
- [20] Lambropoulos P *et al* 2011 *Phys. Rev. A* **83** 021407
- [21] Motomura K *et al* 2009 *J. Phys. B: At. Mol. Opt. Phys.* **42** 221003
- [22] Tiedtke K *et al* 2009 *New J. Phys.* **11** 023029
- [23] Nicolosi P *et al* 2005 *J. Electron Spectrosc. Relat. Phenom.* **144** 1055
- [24] Sorokin A A *et al* 2006 *Appl. Phys. Lett.* **89** 221114
- [25] Feigl T *et al* 2006 *Microelectron. Eng.* **83** 703
- [26] Tiedtke K *et al* 2008 *J. Appl. Phys.* **103** 094511
- [27] Schram B L *et al* 1966 *Physica* **32** 749
- [28] Stockli M P and Fry D 1997 *Rev. Sci. Instrum.* **68** 3053
- [29] Lambropoulos P *et al* 1987 *J. Opt. Soc. Am. B* **4** 821
- [30] Marr G V *et al* 1976 *At. Data Nucl. Data Tables* **18** 497
- [31] Interface to Los Alamos Atomic Physics Codes <http://aphysics2.lanl.gov/tempweb/lanl>
- [32] Verner D A *et al* 1996 *Astrophys. J.* **465** 487
- [33] Kramida A *et al* 2011 *NIST Atomic Spectra Database (ver. 5.0)* <http://physics.nist.gov/asd>